Stereochemistry and size of sugar head groups determine structure and phase behavior of glycolipid membranes: Densitometric, calorimetric, and X-ray studies

8 AUTHORS, INCLUDING:

Rumiana Koynova
The Ohio State University
113 PUBLICATIONS **3,166** CITATIONS

SEE PROFILE

Boris Tenchov
Medical University of Sofia
116 PUBLICATIONS **2,137** CITATIONS

SEE PROFILE

Stereochemistry and Size of Sugar Head Groups Determine Structure and Phase Behavior of Glycolipid Membranes: Densitometric, Calorimetric, and X-ray Studies[†,‡]

H.-J. Hinz,* H. Kuttenreich, R. Meyer, M. Renner, and R. Fründ

Institut für Biophysik und Physikalische Biochemie der Universität Regensburg, Universitätsstrasse 31, D-8400 Regensburg, FRG

R. Koynova, A. I. Boyanov, and B. G. Tenchov

Central Laboratory of Biophysics, Bulgarian Academy of Sciences, 1113 Sofia, Bulgaria

Received August 17, 1990; Revised Manuscript Received January 25, 1991

ABSTRACT: The role carbohydrate moieties play in determining the structure and energetics of glycolipid model membranes has been investigated by small- and wide-angle X-ray scattering, differential scanning densitometry (DSD), and differential scanning microcalorimetry (DSC). The dependence of a variety of thermodynamic and structural parameters on the stereochemistry of the OH groups in the pyranose ring and on the size of the sugar head group has been studied by using an homologous series of synthetic stereochemically uniform glyceroglycolipids having glucose, galactose, mannose, maltose, or trimaltose head groups and saturated ether-linked alkyl chains with 10, 12, 14, 16, or 18 carbon atoms per chain. The combined structural and thermodynamic data indicate that stereochemical changes of a single OH group in the pyranose ring can cause dramatic alterations in the stability and in the nature of the phase transitions of the membranes. The second equally important determinant of lipid interactions in the membrane is the size of the head group. A comparison of lipids with glucose, maltose, or trimaltose head groups and identical hydrophobic moieties has shown that increasing the size of the neutral carbohydrate head group strongly favors the bilayer-forming tendency of the glycolipids. These experimental results provide a verification of the geometric model advanced by Israelachvili et al. (1980) [Israelachvili, J. N., Marcelja, S., & Horn, R. G. (1980) Q. Rev. Biophys. 13, 121–200] to explain the preferences lipids exhibit for certain structures. Generally galactose head groups confer highest stability on the multilamellar model membranes as judged on the basis of the chain-melting transition. This is an interesting aspect in view of the fact that galactose moieties are frequently observed in membranes of thermophilic organisms. Glucose head groups provide lower stability but increase the number of stable intermediate structures that the corresponding lipids can adopt. Galactolipids do not even assume a stable intermediate L_α phase for lipids with short chain length but perform only $L_c \rightarrow H_{II}$ transitions in the first heating. The C_2 isomer, mannose, modifies the phase preference in such a manner that only $L_\beta \rightarrow H_{II}$ changes can occur. Maltose and trimaltose head groups prevent the adoption of the H_{II} phase and permit only $L_\beta \rightarrow L_\alpha$ phase changes. The DSD studies resulted in a quantitative estimate for the volume change associated with the $L_\alpha \rightarrow H_{II}$ transition of 14-Glc. The value of $\Delta \bar{v} = 0.005$ mL/g supports the view that the volume difference between L_α and H_{II} is minute. Analogously, it was found that the enthalpy input required to transform the lamellar L_α phase into the inverted hexagonal structure is only approximately 10% of that of the $L_c \rightarrow L_\alpha$ transition.

One of the challenges of contemporary biochemistry is to unravel the roles of sugar moieties in glycoconjugates. There is a growing awareness that oligosaccharides may be instrumental in mediating such important phenomena as cell–cell recognition (Curatolo, 1987; Hakomori, 1984), interaction with toxins and viruses (Haywood, 1974; Cuatrecasas, 1973), cryoprotection (Womersley et al., 1986; Lis et al., 1990), thermostabilization of cells (Langworthy et al., 1974), and perhaps combined lipid–protein sorting in epithelial cells (Simmons & van Meer, 1988). The actual molecular mechanisms by which these reactions could proceed are far from understood, but certain possibilities suggest themselves. Single sugar moieties and more so oligosaccharides can present a remarkable variety of configurations and structures in relatively short chains by the multiple choices of isomer linkages and branching patterns. The interaction of sugars with water is highly specific and depends strongly on the stereoisomerism

of the hydroxyl groups (Maggio et al., 1985; Kuttenreich et al., 1988). Sugars, particularly in head groups of glycolipids, show a propensity for specific intermolecular hydrogen-bond formation (Pascher & Sundell, 1977; Skarjune & Oldfield, 1979; Hinz et al., 1985), which in principle predestines them for selective communication. Finally, the potent antigenicity of oligosaccharides renders them preferential targets of rapidly elicited antibodies.

This enumeration of the possible roles of sugar moieties in glycoconjugates also illustrates the difficulties encountered in reducing the multiplicity of possible effects to a single or, at least, a small number of interpretable effects in the case where one studies glycolipid extracts from natural membranes (Shipley et al., 1973; Sen et al., 1982; Gounaris et al., 1983; Mannock et al., 1985). Therefore we followed a different strategy for the elucidation of sugar-specific interactions. First, we preferred having homogeneous material that allowed us to single out the specific sugar effects. Second, we tried to establish experimental conditions where the relative contribution of the glyco moieties to the energetics and structure of the lipids was a large enough percentage of the overall effect. The first stipulation can be fulfilled by pure synthetic glycolipids having identical chain lengths but different head groups and the second by a series of glycolipids having identical head groups but alkyl chains of varying lengths. Following these ideas, we synthesized a series of 1,2-*O*-dialkyl-3-*O*-β-D-glycosyl-*sn*-glycerols with 10, 12, 14, 16, or 18 carbon atoms per alkyl chain. The structure, energetics, and phase behavior of the multilamellar vesicles formed by these glycolipids can then easily be related to the stereochemical and size effects of the sugar head groups.

These studies are of relevance to biology, since glycolipids are widely present in tissues of plants (Sastry, 1974), animals (Sweely, 1977), and microorganisms (Ishizuka & Yamakawa, 1985; Ward, 1981). Their biological role is, however, practically unknown. Generally, the lipophilic domains of natural glycolipids are rather similar to those of corresponding phospholipids, while the polar head groups typically show a large diversity. Natural glycolipids comprise mono- and diglucosyldiacylglycerols in *Acheoplasma laidlawii* (Wieslander et al., 1980) and the corresponding galacto compounds in chloroplast membranes (Sen et al., 1981), as well as the highly complex gangliosides (Wiegandt, 1985). The greatest variety of sugar head groups is, however, observed in lipids of archaebacterial membranes that have to exist under extreme conditions of pH and temperature (DeRosa et al., 1986; Langworthy et al., 1982).

In the present study, we were able to demonstrate the important role that the stereochemical configuration of the sugar hydroxyl groups plays in determining the kinetic and energetic phase-transition parameters by comparing gluco- and galactolipids. In order to exclude that the significant differences between these two glycolipids are only characteristic for the C$_4$ isomers of the sugar head groups, we studied a third glycolipid having mannose, the C$_2$ isomer of glucose, as a head group. The results of those studies confirmed the cardinal significance of the stereochemical effects. They showed that the effect of axial compared to equatorial OH groups is dramatically different in different ring positions. We could also separate size effects from stereochemical effects by a comparison of a series of lipids with glucose, maltose, or trimaltose head groups having identical hydrophobic moieties.

The physical parameters used for characterization of the sugar effects are thermodynamic transition parameters, partial specific volumes and volume changes, expansion coefficients,
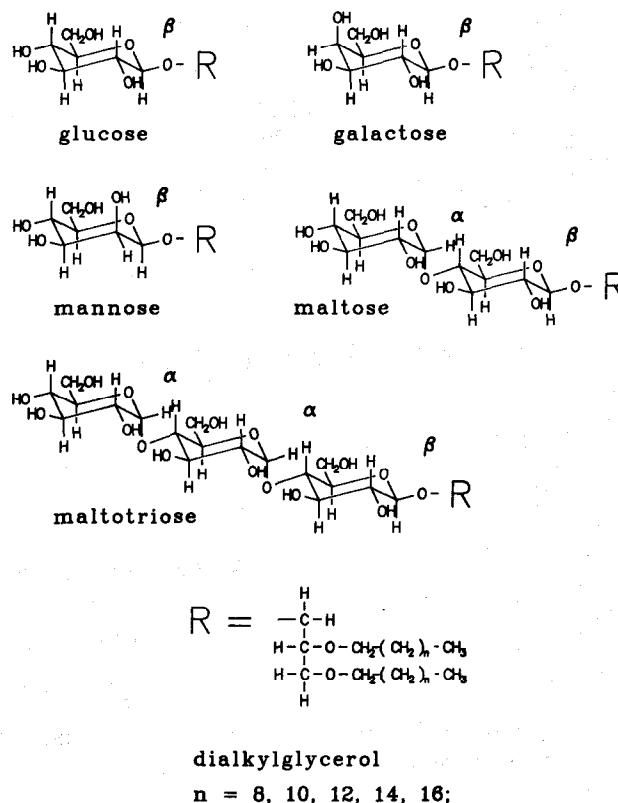

FIGURE 1: Conformational structures of the sugar head groups used in the present studies. The configuration of the dialkylglycerol moieties is shown with (*n* + 2) indicating the length of the saturated alkyl chains.

and structure assignments based on small- and wide-angle X-ray scattering data.

MATERIALS AND METHODS

Materials

1,2-*O*-Dialkyl-3-*O*-β-D-glucosyl-*sn*-glycerols with 10, 12, 14, 16, and 18 carbon atoms in the alkyl chains, 1,2-*O*-dialkyl-3-*O*-β-D-galactosyl-*sn*-glycerols with 12, 14, 16, and 18 carbon atoms in the alkyl chains, 1,2-*O*-dialkyl-3-*O*-β-D-mannosyl-*sn*-glycerols with 14 and 16 carbon atoms in the alkyl chains, 1,2-*O*-dialkyl-3-*O*-β-D-maltosyl-*sn*-glycerols with 14, 16, and 18 carbon atoms in the alkyl chains, and 1,2-*O*-dialkyl-3-*O*-β-D-maltotriosyl-*sn*-glycerol with 14 and 18 carbon atoms in the alkyl chains were synthesized according to a procedure described previously (Six, 1983). Their chromatographic purity was assured by thin-layer chromatography on silica-gel plates (Merck F60 254). Their stereochemical purity and structure were checked by 250-MHz ^{1}H NMR and by ^{13}C NMR, which demonstrated clearly that the aglycon is linked via a β-glycosidic bond to the sugar and additional sugar moieties are connected via α-glucosidic bonds. The molecular weights of the synthetic lipids are as follows: 10-Glc,[1] 534.8; 12-Glc, 590.9; 14-Glc, 647.0; 16-Glc, 703.1; 18-Glc, 759.2; 12-Gal, 590.9; 14-Gal, 647.0; 16-Gal, 703.1; 18-Gal, 759.2; 14-Man, 647.0; 16-Man, 703.1; 14-Mal, 809.1; 16-Mal, 865.2;

---

[1] Abbreviations: 10-Glc, 12-Glc, 14-Glc, 16-Glc, and 18-Glc, 1,2-*O*-dialkyl-3-*O*-β-D-glucosyl-*sn*-glycerol with 10, 12, 14, 16, or 18 carbon atoms per alkyl chain, respectively; 12-Gal, 14-Gal, 16-Gal, and 18-Gal, 1,2-*O*-dialkyl-3-*O*-β-D-galactosyl-*sn*-glycerol with 12, 14, 16, or 18 carbon atoms per alkyl chain, respectively; 14-Man and 16-Man, 1,2-*O*-dialkyl-3-*O*-β-D-mannosyl-*sn*-glycerol with 14 or 16 carbon atoms per alkyl chain, respectively; 14-Mal, 16-Mal, and 18-Mal, 1,2-*O*-dialkyl-3-*O*-β-D-maltosyl-*sn*-glycerol with 14, 16, or 18 carbon atoms per alkyl chain, respectively; 18-Mtr, 1,2-*O*-dioctadecyl-3-*O*-β-D-maltotrisoyl-*sn*-glycerol; PE, phosphatidylethanolamine; DSC, differential scanning calorimetry; DSD, differential scanning densitometry.
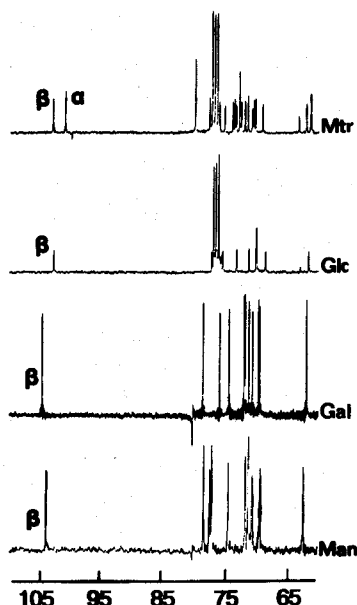
FIGURE 2: ^{13}C NMR spectra of the synthetic glycolipids 18-Glc (Glc), 14-Man (Man), 14-Gal (Gal), and 18-Mtr (Mtr). Measurements on 18-Mtr and 18-Glc were performed in $CDCl_3/CH_3OH$ (5:1 and 9:1, respectively). 14-Gal and 14-Man were measured in methanol. The lipid concentration was 40–80 mg/mL; the resonances labeled β or α refer to the β or α configuration of the C_1' bond of the sugar moieties. The single β resonance of 18-Glc, 14-Man, and 14-Gal, respectively, proves the stereochemical purity of the synthetic lipids. The resonance peak labeled α in the 18-Mtr spectrum has twice the area as the β peak. This clearly demonstrates that we have two $\alpha(1-4)$ links between the sugars in this lipid in addition to the β bond connecting the glycerol with the carbohydrate head group.

18-Mal, 921.4; 14-Mtr, 971.4; and 18-Mtr, 1083.5.

The structures of the head groups of the glycolipids are shown in Figure 1. The ^{13}C NMR patterns that demonstrate the stereochemical purity of the samples are given in Figure 2.

Methods

Sample Preparation. Densitometric and calorimetric measurements required suspensions with concentrations of 10–20 mg/mL and 0.2–0.8 mg/mL, respectively. They were prepared by adding quartz-bidistilled water to weighed amounts of lipid. Sequential cycles of freezing and thawing were performed in combination with vigorous shaking during thawing, with the ice in the vial used as a mechanical homogenizer. This procedure avoids heating above the transition temperature and assures that the suspensions produced in this manner show rather good homogeneity.

Wide- and low-angle static X-ray diffraction studies were performed on 20 wt % suspensions. They were prepared by hydrating the lipids in water for 48 h at room temperature and shaking them with a vortex mixer for 8–10 min at the same temperature.

Density Measurements. Density differences between the lipid suspensions and water were determined by using two DMA 602 HT external cells in combination with a DMA 60 measuring unit (A. Paar, Graz, Austria). Temperature scans between 0.5 and 90 °C were controlled with a Haake PG20 temperature controller and a Haake F3 thermostated bath. The scanning rate was 0.5 °C/min for heating and cooling runs. The temperature was measured with a platinum resistance thermometer placed in a capillary tube in the sample-cell compartment. Temperature readings were made employing a Keithley 195A multimeter.

Data pairs of density and temperature were collected every 0.2 °C with an Olivetti M24 personal computer. Temperature

scans were interrupted for the time of the measurements. Density scans were performed with distilled water in the reference cell and lipid suspensions in the sample cell (Kratky et al., 1973; Laggner & Stabinger, 1976; Koynova & Hinz, 1990). The instrument constant was determined according to the specifications of the producer by using distilled water or air in the sample cell and distilled water in the reference cell. The densities of air and water at corresponding temperatures were obtained from tables in the CRC Handbook of Chemistry and Physics (63rd ed.). Partial specific volumes, $\bar{v}$, of the glycolipids were calculated according to the equation

$$\bar{v} = \frac{1}{\rho_{H_2O}} \cdot \left(1 - \frac{\rho_L - \rho_{H_2O}}{c_L}\right) \qquad (1)$$

where ρ_{H_2O} and ρ_L refer to the densities of water and lipid, respectively, and c_L is the concentration of the lipid in g/mL (Kratky et al., 1973). In principle, the equation is valid only for the determination of the apparent specific volume. However, we did not find any variation with concentration of the apparent specific volume in the concentration range studied, in agreement with literature results (Wiener et al., 1988). Therefore the apparent specific volumes are identical with the partial specific quantities. Transition temperatures and volume changes, $\Delta\bar{v}$, were determined as described by Nagle and Wilkinson (1978). The expansion coefficients α were calculated according to eq 2:

$$\alpha = \frac{1}{\bar{v}} \cdot \frac{\Delta\bar{v}}{\Delta T} \qquad (2)$$

where $\bar{v}$ is the partial specific volume at the specified temperature. $\Delta\bar{v}$ is the volume change occurring in the temperature interval ΔT, i.e., $\Delta\bar{v}/\Delta T$ is the slope of the linear portions of the pre- and posttransitional baselines. Since for many lipids $\bar{v}$ is a linear function of temperature, α can easily be calculated for other temperatures on the basis of the α and $\bar{v}$ values given in Table II.

X-ray Measurements. Ni-filtered CuKα radiation, $\lambda = 1.54$ nm, was used for the X-ray measurements. The low- and wide-angle studies were carried out in a Kratky Compact Camera and a pinhole camera, respectively (both from A. Paar, Graz, Austria) equipped with position-sensitive detectors and Peltier-regulated, temperature-controlled cuvettes. Low-angle studies were made with a detector from M. Braun, Garching, FRG; wide-angle measurements were made with a detector LETI from Inel., Buc, France. The temperature in the sample holder was determined with a Pt 100 resistance probe. The sample-to-detector distance was 26.5 cm for the low-angle and 15 cm for the wide-angle camera. Prior to each measurement the samples were equilibrated at the given temperature for at least 20 min. The data acquisition time was 600 s for the low-angle and between 1000 and 3000 s for the wide-angle measurements. The sample concentration was usually 20 wt %.

DSC Measurements. Microcalorimetric measurements were performed with the use of high-sensitivity DASM-1M or DASM-4 instruments (Privalov et al., 1975). Runs were made in the temperature range of 10–90 °C with heating rates of 0.5 or 1 °C/min. We observed no influence of the heating rate on the thermodynamic parameters. Each sample run was preceded by at least one calibration run to establish the baseline position with solvent (usually distilled and degassed water) in both cells. Heat capacity and temperature data were routinely registered every tenth of a degree by a computer. Lipid concentrations of 0.2–0.5 mg/mL were employed in the measurements. They were determined by weight. Thermo-

Table I: Transition Temperatures (T_m), Partial Specific Volume Changes ($\Delta\bar{v}$), and Enthalpy Changes (ΔH) of the Phase Transformations of the Various Glycolipids, Derived from DSD and DSC Studies (Phase Identification According to X-ray Data)

compound	T_m (°C) ±0.3						$\Delta\bar{v}$ (mL/g) ±10%						ΔH (mL/g) ±10%[a]					
	$L_c{\to}L_\beta$	$L_\beta{\to}L_\alpha$	$L_\beta{\to}L_\alpha$	$L_\alpha{\to}H_{II}$	$L_c{\to}H_{II}$	$L_\beta{\to}H_{II}$	$L_c{\to}L_\beta$	$L_c{\to}L_\alpha$	$L_\beta{\to}L_\alpha$	$L_\alpha{\to}H_{II}$	$L_c{\to}H_{II}$	$L_\beta{\to}H_{II}$	$L_c{\to}L_\beta$	$L_c{\to}L_\alpha$	$L_\beta{\to}L_\alpha$	$L_\alpha{\to}H_{II}$	$L_c{\to}H_{II}$	$L_\beta{\to}H_{II}$
10-Glc		26.2	3.0					0.044	0.031					29.8				
12-Glc		37.3	31.7	56.7[b] / 88.2[c]				0.066	0.026					39.0	15.6	1.1[b] / 0.7[c]		
14-Glc		51.5	51.6	56.4				0.096	0.046	0.005				55.3	24.9	5.3		
16-Glc	57.1					63.4	0.057					0.054	22.9					40.4
18-Glc	56.7					72.5	0.061					0.065	23.3					46.6
12-Gal					59.2	31.7					0.053						45.3[d]	
14-Gal					69.3	52.7					0.085						74.7[d]	
16-Gal					74.2	65.2					0.091	0.042					78.4[d]	26.5[d]
18-Gal					78.3	72.2					0.092	0.062					83.2[d]	29.4[d]
14-Man						48.6					0.052							23.2
16-Man						61.3					0.066							50.6
14-Mal			40.9												27.3			
16-Mal			56.6												40.5			
18-Mal			66.7						0.043						44.8			
18-Mtr			58.1						0.040						54.8			

[a] The values given are average quantities derived from a minimum of three independent measurements (phase identification according to X-ray measurements). [b] These values refer to a $L_\alpha \to Q$ transition. [c] These values refer to a $Q \to H_{II}$ transition. [d] From Kuttenreich et al. (1988).

Table II: The Partial Specific Volumes, $\bar{v}$, and the Expansion Coefficients, α, of the Various Glycolipids As Derived from DSD Measurements

compound	$\bar{v} \pm 0.01$[a] (mL/g)				$\alpha \cdot 10^4 \pm 1.0$[a] (deg^{-1})			
	L_c	L_β	L_α	H_{II}	L_c	L_β	L_α	H_{II}
10-Glc	0.892	0.883 (2 °C) / 0.991	0.960 (50 °C)		10.4		11.2	
12-Glc	0.897	0.930	0.980 (50 °C) / 1.000		3.9	7.1	7.4	
14-Glc	0.890	0.924	1.001 (53 °C)	1.029	4.2	9.4		7.5
16-Glc	0.911	0.934		1.033	2.1	7.4		10.6
18-Glc	0.895	0.937		1.045	2.7	8.0		7.9
12-Gal	0.931			1.004	0.7			7.6
14-Gal	0.922			1.026	1.4			8.6
16-Gal	0.976 / 0.909 (65 °C)			1.000	7.3 (65 °C)			7.9
18-Gal	0.963 / 0.925 (65 °C)			1.029	1.0 / 7.2 (65 °C)			7.4
14-Man		0.908		1.016		11.6		8.4
16-Man		0.922		1.043		9.8		9.5
18-Mal		0.887	0.972			7.1	8.6	
18-Mtr		0.810	0.895			9.6	9.3	

[a] $\bar{v}$ and α values are listed for L_c, L_β, L_α, and H_{II}. Generally the $\bar{v}$ and α parameters refer to 20 °C, if the lipids occur in the L_c or L_β phase. Exceptions, where $\bar{v}$ and α are given for other temperatures, are indicated by temperature values in parentheses. $\bar{v}$ and α values for the L_α and H_{II} phases are reported for 80 °C, exceptions are again specified by temperature values in parentheses. 16-Gal and 18-Gal show a decrease of $\bar{v}$ with increasing temperature. Therefore two $\bar{v}$ values are given, one referring to the temperature before and one after the value decrease.

dynamic quantities were evaluated numerically. Transition temperatures, T_m, refer to the temperature of 50% completion of the phase transition. Due to the very small heat-capacity changes and temperature intervals associated with the phase transitions, linear baselines under the transition peaks were used for enthalpy and T_m calculations. Molar quantities were calculated on the basis of the molecular weights given under Materials.

^{13}C *NMR Measurements.* Spectra were taken on a Bruker MSL-300 spectrometer at 75.4 MHz under continuous proton broad-band decoupling conditions with 45 rf pulses and pulse delays of 3 s. The spectrometer was locked on $CDCl_3$ when this solvent was present. Otherwise the spectrometer was used unlocked, and the ppm scale was referred to the methanol resonance (49.3 ppm). The sweep width was 25000 kHz; the filter width was set to 30000 kHz. A total of 5000 time domain points were accumulated, which, after Fourier transformation, resulted in 16000 data points.

Measurements on 18-Mtr lipids and 18-Glc lipids were performed in a mixture of $CDCl_3/CH_3OH$. The solvent ratio was for these two lipids 5:1 and 9:1, respectively. 14-Gal and 14-Man were measured in methanol. The concentration of the lipids was generally between 40 and 80 mg/mL.

RESULTS

Differential Scanning Densitometry. Partial specific volumes, $\bar{v}$, of the glycolipids as a function of temperature, the volume changes, $\Delta\bar{v}$, resulting from the phase transitions, and the reversibility of these transitions have been determined by DSD studies in the temperature range of 0–90 °C. The parameters obtained by these experiments have been summarized in Tables I and II.

DSD Measurements on Glucolipids. The DSD transition curves of a series of glucolipids having different chain lengths are summarized in Figure 3. During the first heating, 10-Glc and 12-Glc exhibit a single transition at 26.3 and 37.5 °C, respectively (Figure 3a). 14-Glc shows two transitions. The first at 51.6 °C is associated with a volume change of $\Delta\bar{v} = 0.0978$ mg/mL, the second, at 55.1 °C, involves a $\Delta\bar{v}$ more than one order of magnitude smaller than the phase change at 51.6 °C. Both 16-Glc and 18-Glc have two transitions, a
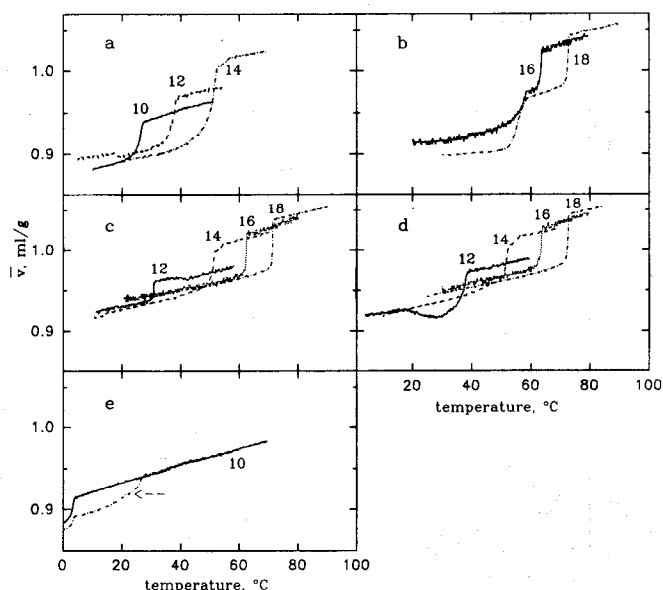
FIGURE 3: DSD scans of monoglucosyldialkylglycerols (Glc's) having saturated alkyl chains of 10, 12, 14, 16, and 18 carbon atoms. The numbers at the curves refer to the alkyl chain lengths. Shown are (a) the first heating of 10-Glc, 12-Glc, and 14-Glc; (b) the first heating of 16-Glc and 18-Glc; (c) the cooling of 12-Glc, 14-Glc, 16-Glc, and 18-Glc; (d) the second heating of 12-Glc, 14-Glc, 16-Glc, and 18-Glc; and (e) the second heating of 10-Glc. The arrow marks the transition curve obtained after keeping the dispersion at 0.2 °C for 10 h. Heating and cooling scans were performed at a scan rate of 0.5 °C/min. The sample concentrations were in the range of 10–20 mg/mL. All traces show original unsmoothed data.

broad transition at 57.5 and 55.8 °C, respectively, and a sharp, more cooperative one at 63.3 °C (16-Glc) and 72.5 °C (18-Glc) (Figure 3b). In cooling scans, only the high-temperature cooperative transitions were observed. In comparison with the first heating, the cooling curves showed a hysteresis of about 1 °C for both the 16-Glc and 18-Glc transitions (Figure 3c). The cooling scans of 14-Glc displayed two transitions at the same temperatures as in the first heating. However, the volume change in the transition at 51.8 °C was only half the value observed in the first heating. 12-Glc undergoes a pronounced volume change at 30.8 °C on cooling. This temperature is 6–7 °C lower than that in the first heating. In addition, a volume increase with decreasing temperature was observed at around 40 °C. With 10-Glc, the transition is shifted to 2 °C on cooling (scan not shown). This transition temperature is 24 °C lower than that obtained in the first heating. The initial transition at 26.3 °C could be partially restored after a 10-h storage at 0.2 °C (Figure 3e).

In the second and following heating and cooling scans, 14-Glc, 16-Glc, and 18-Glc undergo transitions that each are characterized by identical volume changes and transition temperatures for cooling and heating, i.e., the transitions are fully reversible (Figure 3c,d). Only 12-Glc exhibits a more complex pattern. The second heating of the sample is characterized by a pronounced decrease of $\bar{v}$ with increasing temperature starting at about 20 °C and proceeding up to approximately 28 °C. A further temperature increase causes essentially two transitions, the first at 31.7 °C and the second at 37.5 °C. The separation of these two transitions is not obvious in Figure 3d. The two transitions are, however, well resolved in differentiated [(d$\bar{v}$/dT) vs temperature] transition curves.

DSD Measurements on Galactolipids. The DSD transition curves of the galactolipids are exhibited in Figure 4. In the first heating, all four galactolipids exhibit single sharp volume increases, $\Delta\bar{v}$ at transition temperatures, T_m, that increase with
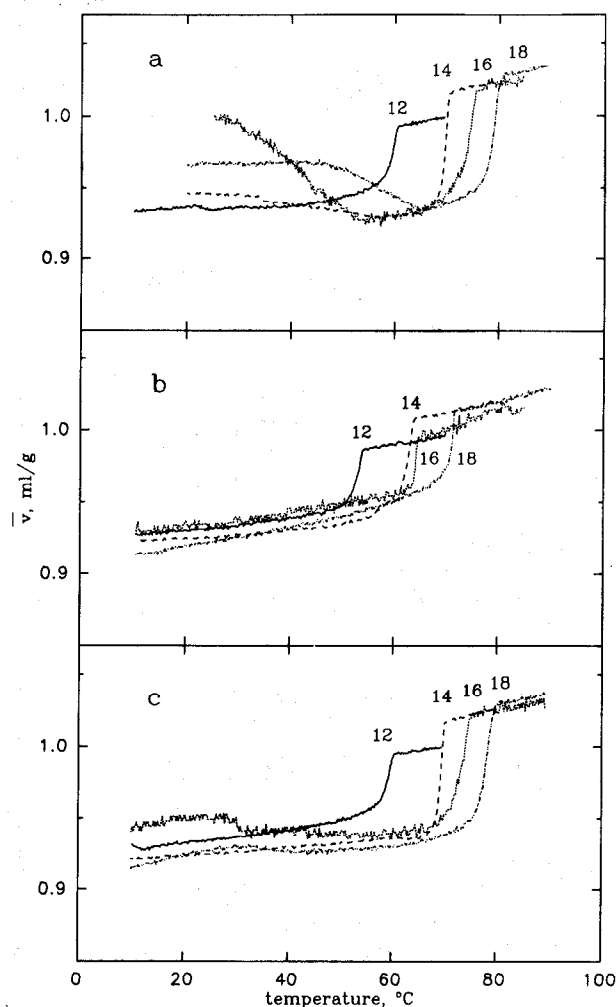

FIGURE 4: DSD scans of aqueous dispersions of monogalactosyldialkylglycerols (Gal's) having saturated alkyl chains of 12, 14, 16, and 18 carbon atoms. The numbers at the curves refer to the alkyl chain lengths. Shown are (a) the first heating of 12-Gal, 14-Gal, 16-Gal, and 18-Gal; (b) the cooling of 12-Gal, 14-Gal, 16-Gal, and 18-Gal; and (c) the second heating of 12-Gal, 14-Gal, 16-Gal, and 18-Gal. Heating and cooling scans were made at a scan rate of 0.5 °C/min. The sample concentrations were between 10 and 20 mg/mL. All traces show original unsmoothed data.

increasing chain length (Figure 4a). The numerical values of T_m, $\bar{v}$, $\Delta\bar{v}$, and α are summarized in Tables I and II. The transition temperatures coincide with those obtained by DSC measurements under the same conditions (Kuttenreich et al., 1988). With all compounds, volume contractions with increasing temperature were observed. This phenomenon was particularly pronounced for 16-Gal and 18-Gal. It is worth noting that the volume decreases do not show up in the heat capacity scans. Either they are zero-enthalpy processes, or, more realistically, these changes involve only low-energy noncooperative processes that are below the limit of detection of the instrument. A possible molecular interpretation of the volume decreases on heating is the following. After low-temperature sample preparation, which avoids drastic mechanical treatment such a sonication, galactolipids form, at least partially, an analogous hydrogen-bond network as found for PE in dry hexane (Sen et al., 1988) or for crystalline PE (Hauser et al., 1981). PE, which is noted for its tendency to form hydrogen bonds between the head groups, shows a similar decrease of $\bar{v}$ with increasing temperature after low-temperature sample preparation (Koynova & Hinz, 1990). The volume contraction with increasing temperature disappears after ultrasound treatment of the PE dispersion at elevated
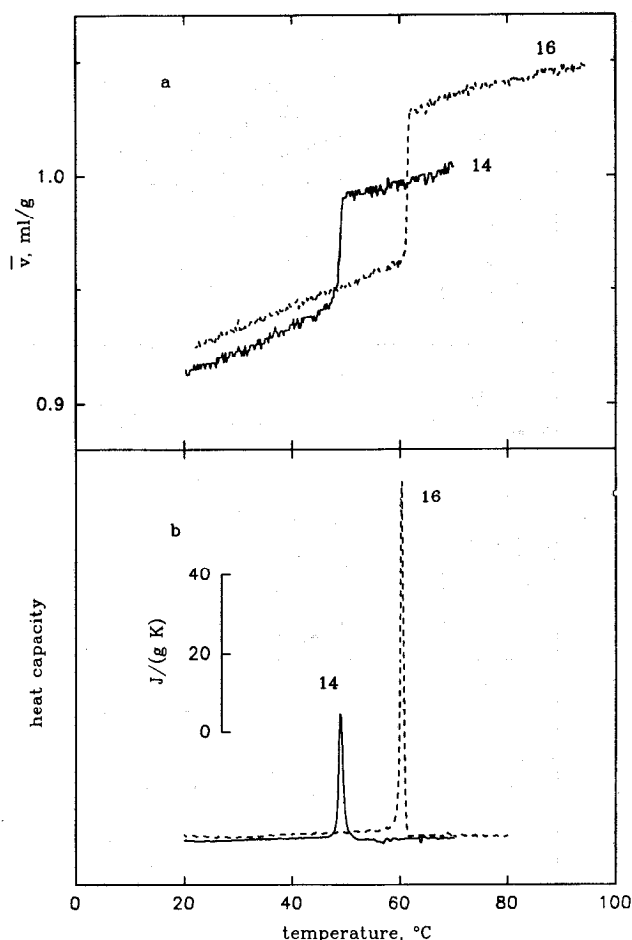
FIGURE 5: DSD (a) and DSC (b) scans of aqueous dispersions of monomannosyldialkylglycerols with chain lengths of 14 and 16 carbon atoms. The densitometric and calorimetric measurements were performed with a heating rate of 0.5 and 1 °C/min, respectively. Sample concentrations were 10–20 mg/mL for the DSD scans and 0.2–0.5 mg/mL for the DSC scans.
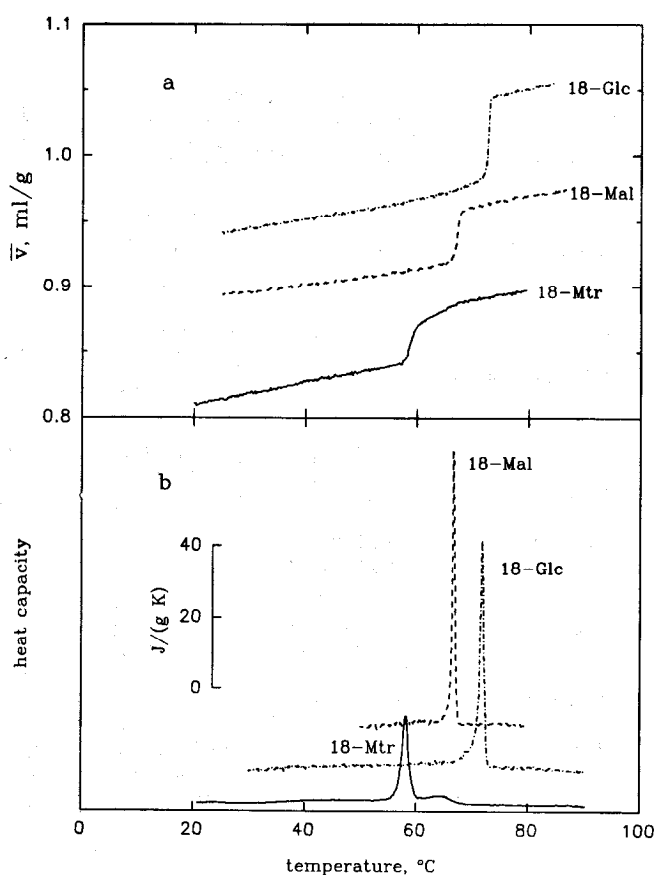
FIGURE 6: DSD (a) and DSC (b) scans of 18-Glc, 18-Mal, and 18-Mtr in water. The curves represent the second heating. The densitometric and microcalorimetric scans were performed with heating rates of 0.5 and 1 °C/min, respectively, with sample concentrations of 10–20 and 0.2–0.5 mg/mL.

temperatures. We conclude that these phenomena observed with both PE and the galactolipids are likely of the same molecular origin. Temperature increase gradually disrupts the bulky hydrogen-bonded structures and thereby causes the volume decreases.

Figure 4b shows the volume changes obtained on cooling. Decreasing the temperature of the 12-Gal, 16-Gal, and 18-Gal suspensions after the first heating leads to single, highly cooperative transitions for all three compounds at temperatures lower by 8–10 °C than in the first heating. 14-Gal (Figure 4b) exhibits a more complex transition behavior. There are two relatively cooperative phase changes visible at 51.4 °C and 60.7 °C. The subsequent second heating restores the original main transitions obtained in the first scan for all lipids, as can be seen from Figure 4c. The pretransitional volume decreases with temperature are, however, not identical with those registered in the first scan. This is an indication of the kinetic origin of some of the low-temperature volume changes.

DSD and DSC Measurements on Mannolipids. Typical DSD- and DSC-transition curves of 1,2-*O*-dialkyl-3-*O*-β-D-mannosyl-*sn*-glycerols with C_{14} and C_{16} alkyl chains (14-Man and 16-Man) are shown in Figure 5. The surprising result of these measurements is that 14-Man and 16-Man each displays only one sharp phase transition that is completely reversible on heating and cooling and also in all subsequent heating–cooling cycles. Calorimetric and densitometric results are in perfect agreement. These results show that the C_2 isomer of glucose strongly suppresses the occurrence of me-

tastability and polymorphism in the model membranes.

Influence of Head-Group Size on the Phase-Transition Properties

Densitometric and Calorimetric Studies. Figure 6a shows the DSD transition profiles determined for 18-Glc, 18-Mal, and 18-Mtr. The transition curve of 18-Glc is taken from Figure 3d. The DSD transition curves of 18-Mal and 18-Mtr are perfectly reversible. This behavior is clearly different from that of 18-Glc, which exhibits two cooperative volume changes on first heating. The 18-Mal transition curve displays a single reversible phase change associated with a volume change at $T_m = 67.2$ °C of $\Delta\bar{v} = 0.0425$ mL/g, while the 18-Mtr transition curve shows a sharp cooperative volume increase of 0.0398 mL/g at 58.6 °C, followed by a noncooperative linear volume increase between approximately 60 and 67 °C. Above that temperature, the regular volume expansion with temperature is observed. Since the only variable in the lipid structure is the number of glucose residues in the head group, the changes in the $\bar{v}$ vs T curves directly reflect the influence of the size of the head group on the phase-transition properties. Furthermore, the series of curves demonstrates very clearly the strong effect of the sugar moiety on the partial specific volume of the lipids. Increasing the relative percentage of carbohydrate in the lipid molecule leads to a considerable decrease of the partial specific volume. This finding can be explained by the additivity of partial specific volumes. Lipids have an average partial specific volume of 1.02 mL/g, sugars a considerably smaller one of 0.61 mL/g (Durchschlag, 1986).

The scanning microcalorimetric studies match the densitometric transition curves perfectly (Figure 6b). The scans

Table III: Low- and Wide-Angle Spacings of Static X-ray Measurements of Various Glycolipids

compound	low-angle spacings (Å)				wide-angle spacings (Å)							
	L_c	L_β	L_α	H_{II}	L_c				L_β	L_α	H_{II}
14-Glc	55.3	56.7	55.8	56.3	4.42	3.81	3.56		4.19	4.42	4.48
18-Glc	62.0	67.2		56.3	4.41	3.83	3.67	3.37	4.07		4.49
14-Gal[a]	54.9	54.9	49.6	54.9	4.51	3.92	3.48				4.50
18-Gal	66.3[b]	67.0		60.9	4.47	3.85	3.48	b	4.14		4.55
16-Man		63.2		54.9					4.15		4.52
14-Mal		65.6	60.3						4.10	4.52	
16-Mal		72.0	63.2						4.07	4.50	
18-Mtr		80.7	69.0						4.15	4.58	

[a] Data from Kuttenreich et al. (1988). [b] Data refer to the L_c phase 60 °C, for comparison see Figure 9.

of 18-Glc and 18-Mal exhibit only one sharp transition peak at transition temperatures identical with those found in the densitometric measurements. Similarly, 18-Mtr shows a transition curve that has a high-temperature shoulder, where the densitograms exhibit the noncooperative volume increase.

DSC Studies of Glucolipids. Phase behavior of a series of glucoglycerolipids after high-temperature sample preparation has been reported previously (Hinz et al., 1985). The calorimetric transition curves observed under those conditions are equivalent to the densitometric transition curves of the second and further heatings obtained in the present study (Figure 3d). So far there existed no studies on suspensions of glucolipids after low-temperature sample preparation that would allow a comparison with the densitometric measurements shown in Figure 3a. Figure 7 reports these microcalorimetric measurements for the same series of lipids that was studied by DSD. Some characteristic features can be seen in the graphs. The transition temperatures of the main endotherms increase with increasing alkyl chain length from 10 to 18. In the transition curve of 12-Glc, two additional peaks appear above the main transition peak at 56.7 and 88.2 °C. 14-Glc shows only one peak a few degrees above the main endotherm but exhibits a pretransition in the form of a low-temperature shoulder of the main endotherm. With 16-Glc only two peaks are visible, a well-separated pretransition and a main transition. 18-Glc shows a still wider separation in temperature of the two transitions. The corresponding transition temperatures and thermodynamic parameters are summarized in Table I. The DSC curves of the glucolipid suspensions obtained in the second and all subsequent heatings were identical with those reported for samples prepared by high-temperature treatment (Hinz et al., 1985). If the suspensions were, however, stored at 2 °C after the first heating for approximately 20 days, partial restoration of the first heating pattern was observed in both calorimetric and densitometric measurements. No systematic study of these slow kinetic phenomena has been undertaken so far.

X-ray Diffraction Studies. The volumetric and energetic changes observed by DSD and DSC are sensitive probes of the phase changes occurring within the bilayers. To gain insight into the molecular details of these structural changes, we performed a large number of small- and wide-angle X-ray scattering studies. Some representative scattering curves obtained at different temperatures are displayed in Figures 8–12. The corresponding low- and wide-angle spacings as well as the phase identifications are summarized in Tables I and III.

Phase Behavior of Glucolipids. Figure 8a summarizes the X-ray patterns of a heating and cooling cycle of 14-Glc and 18-Glc. At 20 °C, prior to the first heating, 14-Glc forms a structure that is characterized by lamellar spacings with a periodicity of 55.33 Å (Table III) and by three pronounced wide-angle reflections at 4.42, 3.81, and 3.56 Å. This pattern is typical for a lamellar lipid bilayer with highly ordered hy-
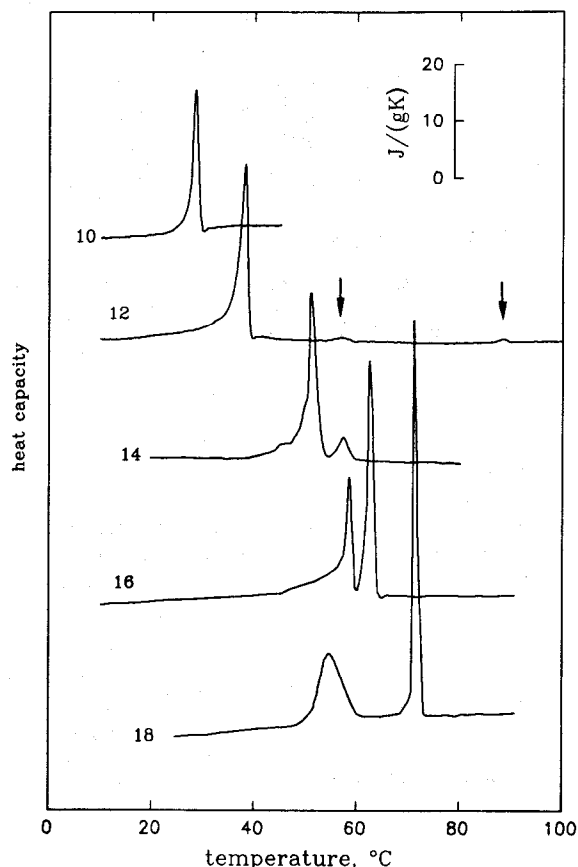

FIGURE 7: DSC scans of 10-Glc, 12-Glc, 14-Glc, 16-Glc, and 18-Glc in water. The transition curves refer to the first heating after low-temperature sample preparation. The arrows at the 12-Glc transition curve indicate the $L_\alpha \rightarrow Q$ and the $Q \rightarrow H_{II}$ transition, respectively. The measurements were performed with a heating rate of 1 °C/min and sample concentrations of 0.2–0.5 mg/mL.

drocarbon chains. Therefore we call it a lamellar crystalline phase, L_c. Heating to 54 °C, through the transition at 51.6 °C, causes the wide-angle reflections to disappear, while the lamellar repeat distance remains practically unchanged. The single broad wide-angle reflection centered at 4.48 Å clearly indicates the appearance of a lamellar L_α phase with melted hydrocarbon chains (Luzatti, 1968). Further heating through the small "posttransition" at 56 °C (see Figure 6) alters the low-angle pattern in a unique manner. Three well resolved reflections at 56.27, 32.87, and 28.37 Å become visible whose spacings show the ratio $1:1/\sqrt{3}:1/2$. Such a ratio in connection with the broad wide-angle peak at 4.58 Å is a clear indication of the occurrence of a hexagonal phase. According to the fundamental studies of Luzatti (1968), an inverted hexagonal H_{II} phase appears to be the most probable structure for a lipid having two alkyl chains per hydrophilic group. Therefore in all subsequent discussion we will use "hexagonal
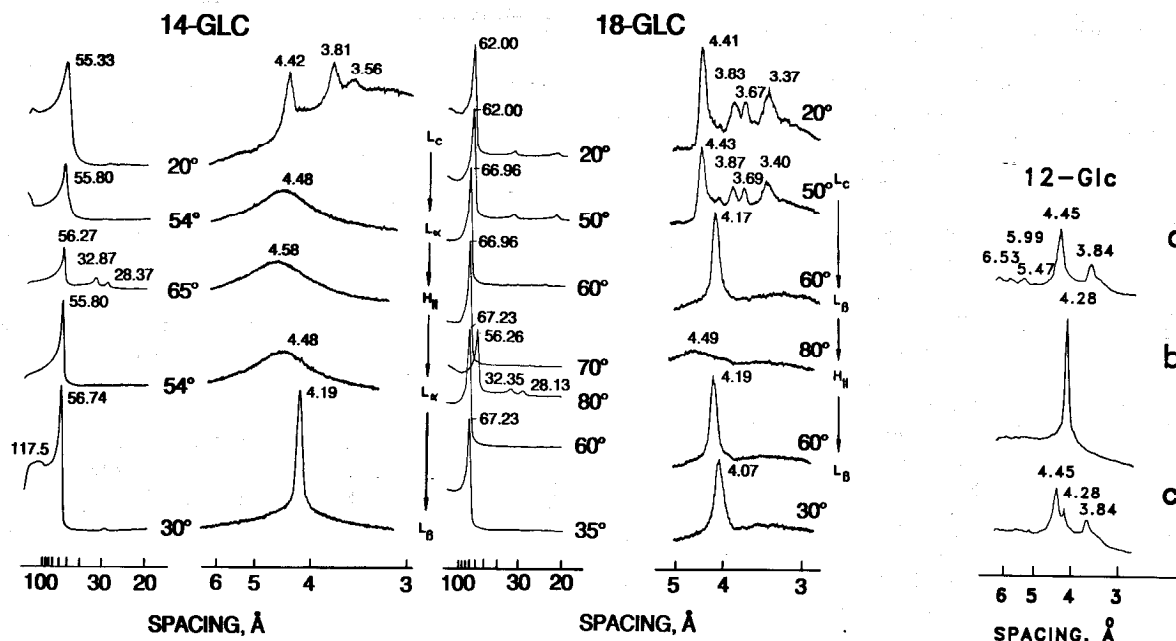
14-GLC

18-GLC

12-Glc

FIGURE 8: (Left and center) Low- and wide-angle diffraction patterns of 14-Glc and 18-Glc determined at temperatures below and above the various phase transitions in heating and subsequent cooling scans. The temperatures and phases are indicated at the diffraction patterns. The sequence of patterns is from top to bottom. (Right) Wide-angle diffraction patterns of 12-Glc in water at 30 °C [T_m ($L_c \rightarrow L_\alpha$) = 37.3 °C; T_m ($L_\beta \rightarrow L_\alpha$) = 31.7 °C]. (a) The first measurement after freeze-thawing. The pattern is that of an L_c phase. (b) The second measurement after heating to 85 °C and cooling to 30 °C (typical L_β pattern). (c) The third measurement after a 12-h incubation at 30 °C. The pattern exhibits the coexistence of L_c and L_β phases.
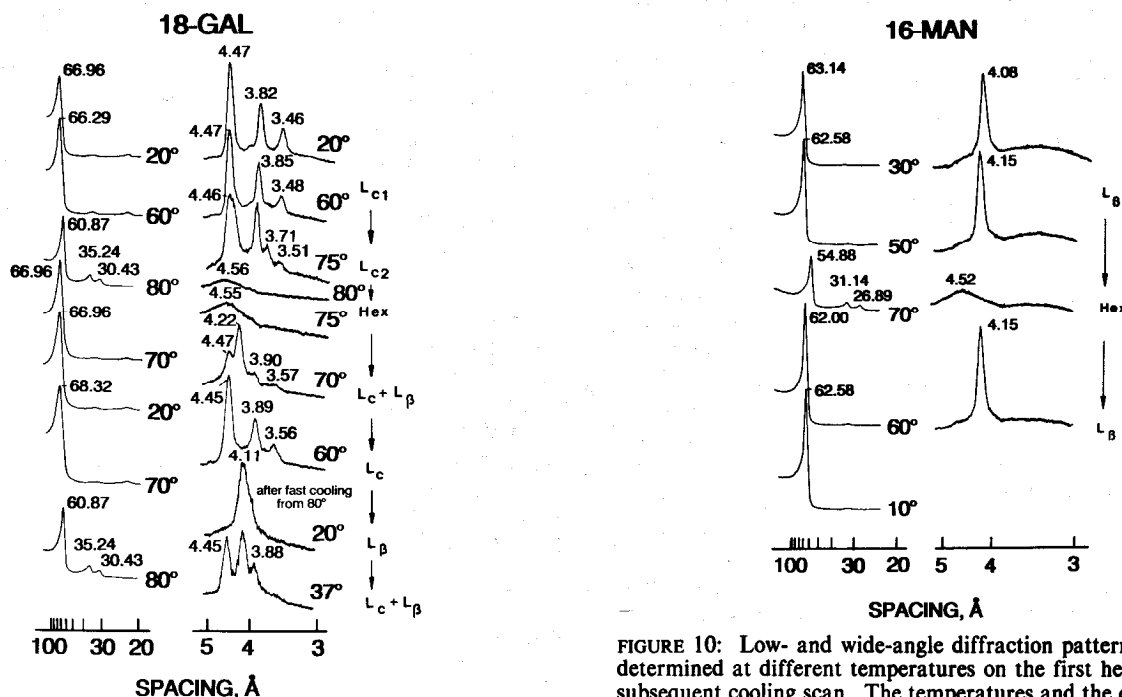
18-GAL

16-MAN

FIGURE 9: Low- and wide-angle diffraction patterns of 18-Gal determined at different temperatures on the first heating and the subsequent cooling scan. The temperatures and the corresponding phases are indicated in the figure. The sequence of patterns is from top to bottom.

FIGURE 10: Low- and wide-angle diffraction patterns of 16-Man determined at different temperatures on the first heating and the subsequent cooling scan. The temperatures and the corresponding phases are indicated in the figure. The sequence of patterns is from top to bottom.

phase" and "H_{II}" synonymously. Cooling from 65 to 54 °C establishes the L_α phase again. However, further decrease of temperature below the transition temperature at 51.5 °C does not regenerate the initially observed L_c phase. The single sharp wide-angle reflection at 4.19 Å together with the low-angle reflection at 56.74 Å unambiguously prove the existence of a hexagonal alkyl chain arrangement within a lamellar L_β phase. Subsequent heatings (not shown) reproduce the sequence of phase changes $L_\beta \leftrightarrow L_\alpha \leftrightarrow H_{II}$. These X-ray data

of 14-Glc correlate perfectly with both the volume and enthalpy changes. During the first heating, the large enthalpy and volume changes are the result of the $L_c \rightarrow L_\alpha$ transformation. Similarly big changes in volume and enthalpy have been found for the $L_c \rightarrow L_\alpha$ transition of PE with 14-carbon chains (Wilkinson & Nagle, 1984; Chowdry et al., 1984; Koynova & Hinz, 1990). In contrast, the $L_\alpha \rightarrow H_{II}$ transition at 56 °C is characterized by 10-fold smaller volume and enthalpy changes. Our values for the volume changes involved in the $L_\alpha \rightarrow H_{II}$ transition are among the few quantitative densitometric parameters published so far. Epand and Epand (1980) did not find measurable volume changes for the liq-
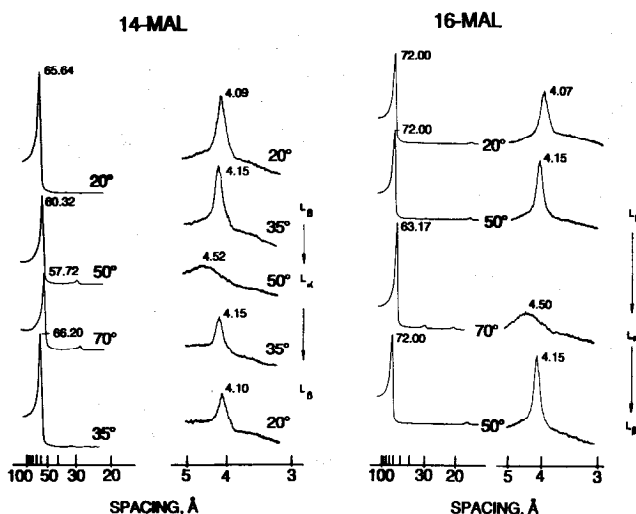
FIGURE 11: Low- and wide-angle diffraction patterns of 14-Mal and 16-Mal determined at different temperatures on the first heating and the subsequent cooling scan. The temperatures and the corresponding phases are indicated in the figure. The sequence of patterns is from top to bottom.
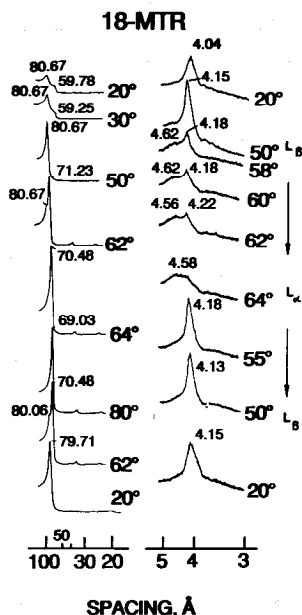

FIGURE 12: Low- and wide-angle diffraction patterns of 18-Mtr determined at different temperatures on the first heating and the subsequent cooling scan. The temperatures and the corresponding phases are indicated in the figure. The sequence of patterns is from top to bottom.

uid-crystal-to-hexagonal phase transition of egg dioleoyl-phosphatidylethanolamines.

The decreased volume changes observed in the densitometric scans on cooling and in the second heating can now easily be rationalized on the basis of the X-ray measurements. Cooling does not restore the L_c phase but leads to the less well-ordered L_β phase. This structural change is associated with 50% smaller volume changes than the $L_c \rightarrow L_\alpha$ transition.

Increase of the alkyl chain length from 14 to 18 carbon atoms apparently improves the van der Waals interactions between the hydrocarbon chains to such an extent that the crystalline lamellar phase assumed by 18-Glc at 20 °C produces four pronounced wide angle reflections at 4.41, 3.83, 3.67, and 3.37 Å. The lamellar repeat distance of 62 Å is typical for a bilayer of fairly extended chains in the trans conformation. Between 20 and 50 °C the wide-angle reflections vary only insignificantly with temperature (Figure 8,

Table I). Heating through the transition at 55.8 °C is associated with an increase of the lamellar repeat distance from 62 to 66.96 Å, and the appearance of a sharp wide-angle reflection at 4.17 Å is characteristic of hexagonal packing of the hydrocarbon chains. This result demonstrates that 18-Glc, in contrast to 14-Glc, changes from L_c to L_β and not to L_α. A further increase in temperature above the transition temperature at 72 °C results in an X-ray picture typical for a H_{II} structure. Different from 14-Glc, in this case the spacings are reduced from 67.23 to 56.26 Å in the $L_\beta \rightarrow H_{II}$ transition. It is worth noting that this periodicity value of 18-Glc in the hexagonal phase is identical with that determined for 14-Glc. Cooling below the transition temperature of 72 °C leads to recovery of the L_β phase. The L_c phase could not be restored within several hours of exposure to room temperature.

This observation is in agreement with the absence of the $L_c \rightarrow L_\beta$ transition at 55.8 °C in DSD and DSC runs of 18-Glc after the first heating. Calorimetric measurements performed on samples that had been kept at 2 °C for 20 days after the first heating revealed only partial restoration of the $L_c \rightarrow L_\beta$ transition peak. Complete transformation of the metastable L_β phase to the stable L_c phase requires, therefore, even longer exposure to low temperature.

We have not performed X-ray studies on 16-Glc. However, the close agreement between the transition properties of 16-Glc and those of 18-Glc as evidenced by DSD and DSC measurements permits the conclusion that this glycolipid exhibits the same phase changes as 18-Glc.

Figure 8b shows wide-angle X-ray studies on 12-Glc to demonstrate the time-dependent recovery of the L_c phase. Measurements at 30 °C before the first heating clearly demonstrate the existence of a highly organized L_c phase (a). After the sample is heated to 85 °C and cooled to 30 °C, the X-ray pattern reveals a pure L_β phase. Storage at 30 °C for 12 h results in the restoration of the original L_c reflections. A small additional peak at 4.28 Å obviously corresponds to a low percentage of L_β phase that has not been converted back to the lamellar crystalline phase.

Phase Behavior of Galacto- and Mannolipids

18-Gal. The complexity of the phase behavior of the galactolipids as well as the simplicity of the phase changes of the mannolipids are reflected in the X-ray diffraction patterns of the lipid dispersions shown in Figures 9 and 10.

At 20 °C 18-Gal forms a highly ordered L_{c1} phase with a bilayer periodicity of 66.96 Å and three prominent wide-angle reflections at 4.47, 3.82, and 3.46 Å. This pattern remains essentially unchanged up to 60 °C. Raising the temperature to 75 °C does not alter the lamellar repeat distance but generates an additional wide-angle reflection at 3.71 Å.

The appearance of this reflection indicates changes in the packing mode of the hydrocarbon chains. Similar changes were observed with 14-Gal in the first heating after low-temperature sample preparation (Kuttenreich et al., 1988). Since the conformational changes take place between two lamellar crystalline phases, we designate them L_{c1} and L_{c2}. Neither with 14-Gal nor with 18-Gal did we find heat capacity anomalies in the calorimetric transition curves that could be assigned to these structural rearrangements between the two crystalline lamellar phases. It may be possible, however, that the gradual, noncooperative negative volumes changes apparent in the DSD measurements in Figure 4 are correlated with these changes in the packing mode.

Further heating through the transition at 78.3 °C results, at 80 °C, in the characteristic pattern of the H_{II} phase, with molten hydrocarbon chains indicated by the broad 4.56-Å

wide-angle reflection and the three low-angle reflections showing the ratio $1:1/\sqrt{3}:1/2$. The transition to the hexagonal phase is associated with a reduction in the periodicity from 66.29 Å (at 60 °C) to 60.87 Å (80 °C). A similar reduction was also found for 18-Glc. On cooling, at 75 °C 18-Gal is still in the hexagonal phase, as demonstrated by the identity of the wide-angle pattern, but at 70 °C a mixture of L_c and L_β phases already coexists. The repeat distance has increased again to 66.98 Å, and the wide-angle reflections are a mixture of the three reflections of the crystalline phase and the one of the L_β phase. A further decrease to 60 °C (low-angle pattern not shown) and to 20 °C (wide-angle reflections not shown) results in full recovery of the L_c phase. If the sample is quenched from 80 to 20 °C within 2 min (indicated as "fast cooling" in Figure 9), the single wide-angle L_β reflection at 4.17 Å signals the absence of crystalline L_c phases. Recrystallization can be achieved by heating the dispersion to 37 °C. At this temperature, a mixture of wide-angle reflections (4.45, 3.88, and 4.11 Å) appears that is indicative of coexisting L_c and L_β phases. On further heating, the crystalline structure is fully recovered, and it melts at 80 °C into the hexagonal phase, as the low-angle pattern demonstrates.

Generally, one can state that different cooling procedures and equilibration times at low temperature result in 18-Gal mixtures that contain different ratios of L_β and L_c phases. On heating above 40 °C, all mixtures are converted to a single crystalline L_c phase. These results are in excellent agreement with the transition scheme proposed for galactolipids on the basis of our previous calorimetric studies (Kuttenreich et al., 1988). They provide the X-ray evidence for the correctness of our previous interpretation of the exothermic peak around 40 °C as being indicative of a relaxation into an highly ordered crystalline phase. In the present X-ray studies, we failed to identify the phase change responsible for the single endotherm at about 72 °C obtained in the previous study (Kuttenreich et al., 1988, Figure 3b,e,i). This negative result is an indication of the kinetic origin of the stability of that phase.

16-Man. The diffraction pattern of 16-Man (Figure 10) is extremely simple in comparison to the diagrams of the gluco- or galactolipids. Obviously, replacing glucose by mannose as head group causes the disappearance of the polymorphism. The diffraction pattern indicates the existence of a lamellar gel phase, L_β, below the transition temperature of 61 °C that shows a bilayer periodicity of about 62 Å and a hexagonal phase above 61 °C with reduced spacings of 54.88 Å at 70 °C. The transition is fully reversible in agreement with the results of the DSD and DSC studies.

Influence of the Size of the Head Group on the Phase Transition Properties of Glycolipids. Figure 11 shows the diffraction pattern of 14-Mal and 16-Mal, Figure 12 that of 18-Mtr. The inclusion of the two maltose-containing lipids with different alkyl chain lengths serves to demonstrate that the simplicity of the phase changes is determined by the head group rather than by the alkyl chains. Both 14-Mal and 16-Mal exhibit reversible $L_\beta \leftrightarrow L_\alpha \leftrightarrow L_\beta$ phase changes in heating–cooling cycles. Transformation from L_β to L_α is accompanied by a reduction in the bilayer periodicity from approximately 65 to 60 Å for the 14-Mal compound and from 72 to 63 Å for the 16-Mal lipid.

The X-ray patterns of 18-Mtr, which has three glucose moieties as a head group, are slightly more complex. The general sequence of reversible phase changes is also $L_\beta \leftrightarrow L_\alpha \leftrightarrow L_\beta$. However, in the first heating at 20 °C, two low-angle reflections are observed at 80.67 and 59.78 Å together with a wide-angle reflection at 4.04 Å. This pattern is practically still the same at 30 °C (80.67, 59.25, and 4.04 Å) (wide-angle pattern not shown). We interpret these reflections as being indicative of the coexistence of two β phases after low-temperature sample preparation. The reason for their occurrence could stem from differences in the degree of hydration of the large sugar head group.

Heating to 50 °C leads to a unique lamellar gel structure, L_β, with a repeat distance of 80.67 Å and a wide-angle reflection at 4.15 Å. Further heating to temperatures above the transition at 58 °C generates a lamellar liquid-crystalline L_α phase with a repeat distance of 70.48 Å at 64 °C. Since both densitometric and calorimetric measurements had not shown symmetric transition curves but gave indications of high-temperature shoulders, we performed X-ray measurements at temperatures inside the transition region. The wide-angle patterns at 58, 60, and 62 °C and the low-angle picture at 62 °C are included in Figure 12. Inspection of these patterns reveals that the low-temperature gel phase (L_β) and the liquid-crystalline phase (L_α) coexist in the transition range shown by the DSD and DSC measurements. Cooling to 20 °C gives rise to a single L_β phase with a bilayer periodicity of 79.71 Å.

Discussion

In the present study we have tried to lay a sound foundation of structural and thermodynamic parameters that might be conducive to better understanding and appreciation of the role carbohydrate head groups play in governing the structure and stability of glycolipid model membranes. The dramatic dependence on the configuration of the hydroxyl groups in the sugar ring of the nature and the energetics of the phase changes can be used as a paradigm for their possible influence in biological membranes. It may also serve as an example for the general type of interactions that sugar moieties in glyco-conjugates can get involved in. While we used temperature increase as the most convenient parameter to probe the structural propensities of the various glycolipids, analogous changes are likely to be induced by all other factors that perturb the balance of forces between head groups and the hydrophobic part of the molecules. The synthesis of selected glycolipids that contain only variations in the head group structure or, alternatively, in the length of the hydrocarbon chains allowed us to differentiate unambiguously between head-group effects and van der Waals effects of the hydrocarbon chains. Since all methods employed in characterizing the glycolipid structures and their changes were noninvasive, we need not worry about possible interference from imported probe perturbations.

Position and Orientation of OH Groups in the Hexose Head Group Determine the Phase Behavior of Glycolipids

Stereochemical Effects of OH Groups in Different Ring Positions: (A) Effects in the C4 Position. The structure and the phase transitions of glycolipids in aqueous dispersions are the result of a delicate balance between head-group and chain-length effects. The overall head-group effect is the resultant of the positional effect of the hydroxyl group and its stereochemical effect due to isomerism. Thus it is important not only whether an OH group occurs axially or equatorially but also on which C atom in the pyranose ring the OH group is located. This conclusion holds for all asymmetric C atoms including the anomeric C atom at position 1. Studies by Jarrel et al. (1987) on α-14-Glc revealed that both the head-group orientation and the molecular ordering in the lamellar and hexagonal phases are strikingly different from those of the β-anomer. To avoid complications from the anomeric linkage,
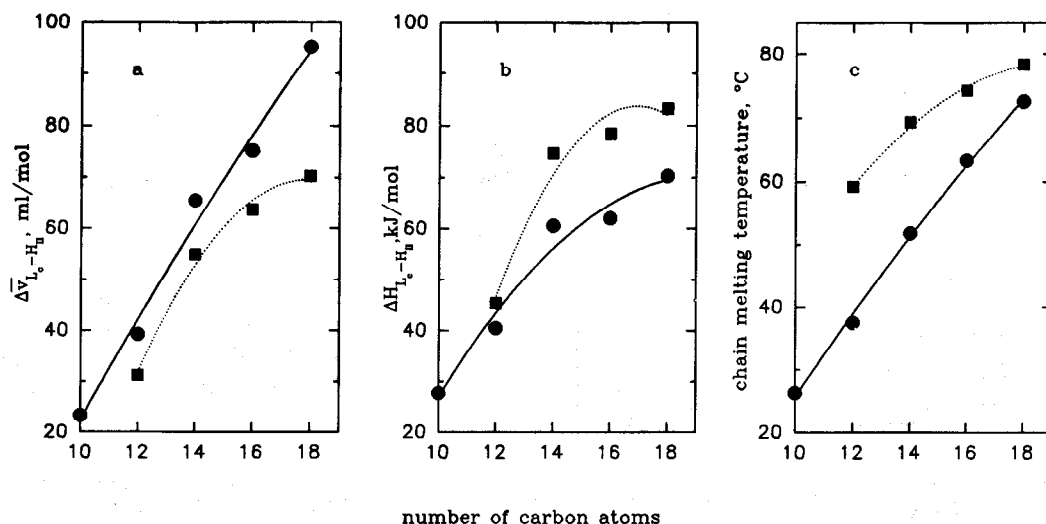
FIGURE 13: Comparison of the thermodynamic transition parameters (a) $\Delta\bar{v}_{L_c-H_{II}}$, (b) $\Delta H_{L_c-H_{II}}$, and (c) the chain-melting temperature for glycoglycerolipids having glucose and galactose head groups. Values for different alkyl chain lengths have been given. The volume changes were determined by DSD measurements and the enthalpies and the transition temperatures by microcalorimetry. Solid points refer to glucolipids and solid squares to galactolipids. The error limits of the data are given in Tables I and III. For galactolipids that exhibit only the $L_c \rightarrow H_{II}$ transition the $\Delta\bar{v}$ values in panel (a) result directly from the DSD scan. For glucolipids, the $\Delta\bar{v}$ value is the sum of the volume changes of all intermediate transitions. The $\Delta\bar{v}$ values of 10-Glc and 12-Glc refer only to the $L_c \rightarrow L_\alpha$ transitions in the first heating. We imply that they will be only minutely smaller than the $\Delta\bar{v}_{L_c-H_{II}}$ values. The ΔH value for 10-Glc in panel (b) is assumed to result from the $L_c \rightarrow L_\alpha$ transition in analogy to the structural changes observed with 12-Glc as a function of temperature. As was shown experimentally for the $L_\alpha \rightarrow H_{II}$ transition of 12-Glc, the overall phase change from L_α to H_{II} is associated with a ΔH of 1.8 kJ/mol (Table I). We assume, therefore, that the error involved in equating $\Delta H_{L_c-L_\alpha}$ with $\Delta H_{L_c-H_{II}}$ (if such a transition exists) is negligible. The transition temperatures in panel (c) refer to the chain-melting transition in the first heating. Since chain melting is associated with the $L_c \rightarrow H_{II}$ transition for all galactolipids, the solid squares refer to that structural change. Chain melting in glucolipids is connected with different phase changes. Therefore, the temperature values refer to the following phase transitions, respectively: 10-Glc, 12-Glc, and 14-Glc, $L_c \rightarrow L_\alpha$; and 16-Glc and 18-Glc, $L_\beta \rightarrow H_{II}$.

we synthesized only glycolipids with the β configuration at C_1. Figure 13 summarizes the different effects of glucose and galactose head groups on the thermodynamic transition parameters of glycolipids with various chain lengths. Overall molar volume changes, $\Delta\bar{v}$, molar transition enthalpies, ΔH, and the transition temperatures for the chain-melting transitions, T_m, have been plotted versus the number of carbon atoms in the alkyl chains. The transition enthalpies shown in Figure 13b refer to $L_c \rightarrow H_{II}$ transition. All galactolipids exhibit only the $L_c \rightarrow H_{II}$ phase change in the first heating. Therefore these enthalpy data can be directly obtained from the heat capacity transition peaks in the first scan. With glucose as a head group, the transitions are no longer as simple. In the first heating after low-temperature sample preparation, the following transitions can be observed: 10-Glc, $L_c \rightarrow L_\alpha$; 12-Glc, $L_c \rightarrow L_\alpha \rightarrow Q \rightarrow H_{II}$; 14-Glc, $L_c \rightarrow L_\alpha \rightarrow H_{II}$; 16-Glc, $L_c \rightarrow L_\beta \rightarrow H_{II}$; and 18-Glc, $L_c \rightarrow L_\beta \rightarrow H_{II}$. Molten chains occur in either the L_α or H_{II} phase. The corresponding chain-melting transition temperatures employed in the construction of Figure 13c for the glucolipids refer to the $L_c \rightarrow L_\alpha$ phase change for 10-Glc, 12-Glc, and 14-Glc and to $L_\beta \rightarrow H_{II}$ for 16-Glc and 18-Glc. The volume changes plotted in Figure 13a refer to $L_c \rightarrow H_{II}$ phase transformations. They are, in the case of glucolipids (solid points), the sums of all intermediate volume changes, whenever these have been measured. The $\Delta\bar{v}$ values employed for 10-Glc and 12-Glc are those of the $L_c \rightarrow L_\alpha$ transition. They have been used under the assumption that due to the very small $\Delta\bar{v}$ change associated with the $L_\alpha \rightarrow H_{II}$ transition (see value for 14-Glc in Table I) this neglection introduces only a minor error. Similar considerations apply to the choice of ΔH values plotted in Figure 13b for the glucolipids as a function of alkyl chain length. With the exception of the parameters for 10-Glc, all ΔH values refer to the sum of the ΔH of all intermediate transitions. The ΔH value plotted in Figure 13b for 10-Glc is that determined for the $L_c \rightarrow L_\alpha$ transition, again assuming

that this ΔH value is only minutely smaller than that for a $L_c \rightarrow H_{II}$ phase change. The striking conclusion one has to draw from these results is that a single hydroxyl group in either the equatorial (Glc) or axial (Gal) position can dramatically alter the stability and the nature of the structural transitions in glycolipid model membranes. While with glucolipids the normal, almost linear, increase of stability (T_m), enthalpy, and partial specific volume changes ($\Delta\bar{v}$) with increasing alkyl chain lengths are observed, galactose head groups introduce a pronounced nonlinearity. This is reflected in the obvious tendency for saturation of all three characteristic thermodynamic quantities of galactolipids (Figure 13). One objection could be raised against the above comparison. The $\Delta\bar{v}$ values of 10-Glc and 12-Glc employed in Figure 13a and the ΔH value of 10-Glc employed in Figure 13b refer to a $L_c \rightarrow L_\alpha$ transition and not to a $L_c \rightarrow H_{II}$ transition. Therefore it may appear questionable to use these values for the comparison between gluco- and galactolipids. Though this objection is valid in principle, inspection of Table I reveals that the major event governing both the volume increase and the transition enthalpy is the chain-melting transition. Once the chains have acquired motional freedom in the L_α phase, further rearrangement to the hexagonal phase involves only very small volume changes (14-Glc: $\Delta\bar{v} = 0.005$ mL/g) and correspondingly small enthalpy changes (14-Glc: $\Delta H = 5.3$ kJ/mol). Therefore, the inclusion of the two short-chain lipids into the comparison appears to be justified. On the basis of the present results, it is worth emphasizing that glycolipids have an enormous capacity of influencing the structure and stability of membranes by stereochemical differentiation.

(B) *Effects in the C2 Position.* A comparison of the structural and thermodynamic data of galacto-, gluco-, and mannolipids having identical chain lengths shows the dependence of the stereochemical effect on the OH group in different ring positions. Converting an equatorial OH group into an axial one at the C_2 position disposes of all polymorphism
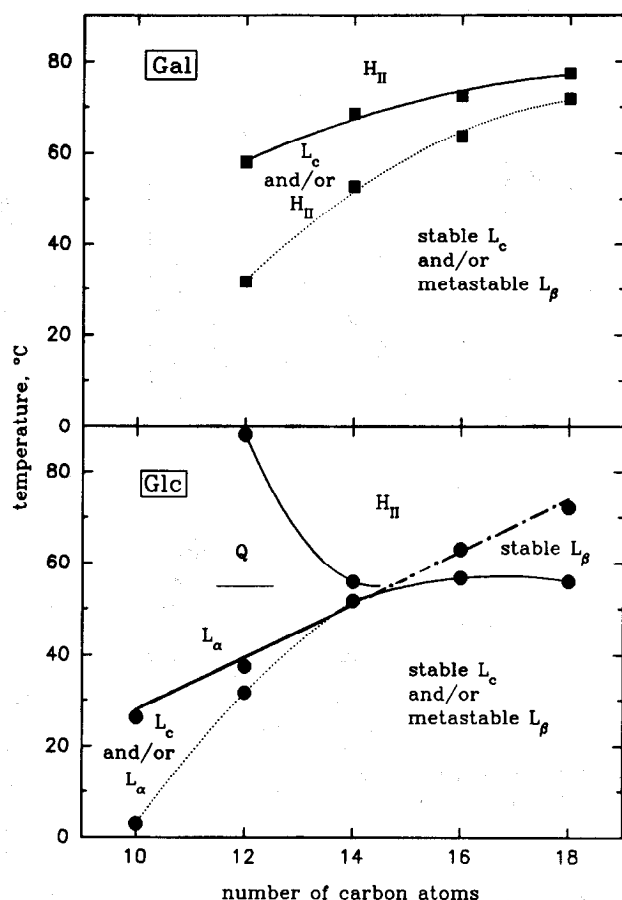
FIGURE 14: Comparison of the phase behavior of glycoglycerolipids having glucose and galactose head groups. The transition temperatures were derived from calorimetric measurements [Kuttenreich (1991) Ph.D. Thesis, University of Regensburg, FRG]. Phase identification was done by small- and wide-angle X-ray scattering studies as discussed in the text. The solid lines connect transition temperatures that are obtained in the first heating after low-temperature sample preparation. Dotted lines refer to transition temperatures determined in the second heating. In the Glc panel, the $L_\beta \rightarrow H_{II}$ transition temperatures observed in the second heating are identical with those obtained in the first heating. Therefore that part of the graph is dash–dotted.

characteristic of glucolipids and galactolipids and causes the L_β structure to be the most stable low-temperature phase of mannolipids. This result is rather extraordinary, because for the glucolipids the L_β phase is either never stable (12-, 14-Glc) or only marginally stable in a small temperature range (57–63 °C for 16-Glc; 56–72 °C for 18-Glc). For the galactolipids, the L_β phase is always a metastable phase. This is demonstrated in Figure 14, where the transition temperatures and the corresponding stable and metastable phases of the various glucolipids (lower half) and galactolipids (upper half) have been summarized. It is apparent that the stable low-temperature phase of all glucolipids is L_c. This conclusion is based on X-ray evidence (Figure 8b) and on the experimental finding by DSD and DSC of a partial reappearance of the $L_c \rightarrow L_\beta$ transition after prolonged low-temperature equilibration following the first heating. However, it is also supported by the general behavior of other lipids exhibiting polymorphism, such as saturated PEs (Koynova & Hinz, 1990) or galactolipids (Kuttenreich et al., 1988; Koynova et al., 1988). In these cases, it has been observed that identical phase transitions result from lipid suspensions independent of their preparation below or above T_m, provided that the lipids prepared at high temperature are exposed to low temperature for a long enough period of time before the measurement. Formation of L_β depends on the conditions and the thermal history of the sample. The

kinetics of relaxation into the more stable L_c phase are rather slow, which permits detection of pure L_β phases in the time course of the calorimetric, density, and X-ray measurements. Galactolipids can also form L_β phases (Figure 14, upper half), but their instability is even greater. A temperature of about 40 °C in the second heating is high enough to overcome the activation barrier that prevents formation of the L_c phase at lower temperatures. The relaxation times for the $L_\beta \rightarrow L_c$ transition of a given lipid class at lower temperature are roughly proportional to the hydrocarbon chain length, as has already been demonstrated in previous studies (Kuttenreich et al., 1988; Seddon et al., 1983). It is worth recalling that both transition enthalpies and temperatures of the $L_c \rightarrow H_{II}$ transition are higher for galactolipids than for glucolipids. However, the corresponding volume changes are larger for the glucolipids. The property of the galactose head groups to impart higher stability (T_m) and higher energetic interactions (ΔH) to glycolipid membranes has been observed in previous studies (Kuttenreich et al., 1988; Koynova et al., 1988). The molecular basis of these differences between glucose and galactose head groups is probably the lower degree of hydration of the latter (Kuttenreich and Hinz, paper in preparation). A smaller number of solvating water molecules per sugar moiety would keep the head-group volume small and thereby interfere minimally with optimization of the van der Waals interactions between the hydrocarbon chains. Furthermore, hydrogen-bond formation between the sugar moieties may be favored by a lower level of local hydration. The strong effect of the configuration of the OH group in position 2 of the pyranose ring on the phase behavior of the glycolipids is intriguing. Crystalline phases are no longer accessible for mannolipids, and the kinetics of the L_β to H_{II} transition are fast enough to prevent the occurrence of metastable states. These results on the positional effects of the OH groups clearly demonstrate the intricacies of sugar–solvent and sugar–sugar interactions and the poor understanding of their molecular basis.

Increasing Size of Neutral Carbohydrate Head Groups Favors a Bilayer-Forming Tendency. Inspection of the transition data for the glycolipids with a monosaccharide head group shows that the stable high-temperature structure is the H_{II} phase (Table I). Introduction of a disaccharide (maltose) or a trisaccharide (trimaltose) moiety completely suppresses the ability to form nonbilayer structures. The lamellar liquid-crystalline (L_α) phase has now become the most stable high-temperature phase. This drastic change in transition characteristics is identical for 14-Mal and 16-Mal as demonstrated in Figure 11. The independence of this effect from the increase in chain length is a strong indication of a dominating influence of the size of the head group on the structural organization of the lipid chains. Our results can be used to test the theoretical models advanced by Israelachvili (1980) for the prediction of the type of structure different lipids will assemble into. A dimensionless "packing parameter" $v/(a_0 \cdot l_c)$ has been derived, whose value is diagnostic of whether the lipids form spherical micelles ($v/(a_0 \cdot l_c) < 1/3$), nonspherical micelles ($1/3 < v/(a_0 \cdot l_c) < 1/2$), or bilayers ($1/2 < v/(a_0 \cdot l_c) < 1$). The parameter a_0 is the socalled "optimal surface area" per molecule, v the volume of the hydrocarbon chains, and l_c the critical chain length. As a_0 parameters, we used the surface area of the respective lipids (14-Glc, 41 Å²; 14-Mal, 45 Å²; 14-Mtr, 50 Å²), which was determined by Langmuir studies (Six, 1984). The parameters v and l_c were calculated according to Tanford (1972) and Israelachvili (1976) by using the formulae $v \approx [27.4 + 26.9 \cdot 2 \cdot (n - x)]$ and $l_c \approx [(1.5 +$

1.265·$(n - x)$], with $x = 0$ or 2 and n being the number of CH_2 groups per alkyl chain. The packing parameters obtained for the series of 14-Glc, 14-Mal, and 14-Mtr are 0.991, 0.883, and 0.813, respectively, when $x = 0$ is employed in the formulae for v and l_c. Since actually the critical length, l_c, is a semi-empirical parameter, which represents a somewhat vague cut-off distance beyond which hydrocarbon chains can no longer be considered as fluid, it was suggested to use not the full length n of the hydrocarbon chains, but a reduced length $(n - 2)$ (Israelachvili et al., 1976). However, the packing parameters obtained in this fashion are not significantly different (0.984, 0.877, and 0.807) from those calculated on the basis of the full alkyl chain length. The agreement with the predictions of the theory is excellent. A packing parameter >1 is supposed to indicate formation of inverted micelles, while values between 0.5 and 1 are suggestive of bilayer formation. The value for 14-Glc is so close by 1 that slight changes in l_c and a_0, which will occur with increasing temperature, are likely to render the packing parameter >1. Such a value would then be compatible with the formation of an H_{II} phase. Indeed, we found that for 14-Glc the transition sequence is $L_c \rightarrow L_\alpha \rightarrow H_{II}$. The two other lipids fit equally nicely into the picture. By the increase of the head-group area, a_0, the packing parameter drops to values characteristic of a bilayer-forming tendency. Experimentally 14-Mal and 14-Mtr have been found to exist only in lamellar structures even at high temperature. Analogous calculations applied to 18-Glc, 18-Mal, and 18-Mtr result in the following numbers for the packing parameter: 1.000, 0.892, and 0.820. The full number of carbon atoms has been used to calculate v and l_c, and the same a_0 values as for the C-14 lipids have been assumed. Again the experimental results are in accord with the predictions of the model which states that, according to the value of the packing parameter, 18-Glc is the only lipid that can be expected to form nonbilayer structures. In addition to providing a verification of these geometric considerations, our studies give an energetic description of the effect resulting from the increase of the size of the head group. They show that the stability of the L_β phase decreases strongly with increasing head-group size, as is indicated by the decrease in T_m, and that this decrease in stability is not paralleled by a corresponding decrease in the transition enthalpy. A calculation of the transition entropies for the $L_\beta \rightarrow L_\alpha$ transition of 18-Glc, 18-Mal, and 18-Mtr yields the values 118.3, 126.5, and 175.4 J/(mol·K), respectively. These data imply that an increase in the size of the carbohydrate moiety is associated with a favorable molar entropy gain in the $L_\beta \rightarrow L_\alpha$ transition. In calculating the ΔS value for the $L_\beta \rightarrow L_\alpha$ phase change of 18-Glc from our enthalpy value for the $L_\beta \rightarrow H_{II}$ transition, we used the enthalpy value ΔH ($L_\alpha \rightarrow H_{II}$ = 6.1 kJ/mol reported by Mannock et al. (1988). These authors determined the value in their excellent systematic study on acylgluco-glycerolipids. Since it is known that possible differences between lipids having acyl- or ether-linked alkyl chains are small (Ruocco et al., 1985; McKeone et al., 1986), we probably do not introduce significant errors into the entropy calculation by this choice. The favorable entropy gain and the lower stability resulting from the increase in the size of the head group can be rationalized by assuming an increased number of vibrational and rotational degrees of freedom of the hydrocarbon chains after melting. Although nothing is known about the exact orientation of the maltose and trimaltose moieties at the hydrocarbon water interphase, the Langmuir measurements mentioned above have shown an increasing space requirement of the head groups in proportion to the

number of glucose moieties. The wider separation of the alkyl chains in bilayers of lipids with large head groups compared to those with small head groups can be envisaged to result in correspondingly greater conformational freedom of the chains in the L_α phase. This would explain both the entropy gain and the lower stability.

Modulation of Chain-Length Effects by Sugar Head Groups. It is quite obvious that the relative contribution of the sugar head groups decreases with increasing alkyl chain length. The decrease is not proportional to chain length, as has been mentioned before. The nonlinearity can be understood when the complex changes in polymorphic behavior apparent in the calorimetric and X-ray studies are taken into account. Figure 14 summarizes the different changes generated in the transition behavior by glucose and galactose head groups at a variety of chain lengths. It is noteworthy that even with a chain length of 10 glucolipids still form a bilayer structure, whose transitions, in analogy to the phase changes observed with 12-Glc, can be ascribed to an $L_c \rightarrow L_\alpha$ transition on first heating and to an $L_\beta \leftrightarrow L_\alpha$ change on cooling. Though the X-ray evidence is lacking, both calorimetric and density studies support this conclusion. 12-Glc exhibits two high-temperature transitions at 56 and 88 °C that, according to our preliminary time-resolved X-ray studies, can be identified as $L_\alpha \rightarrow Q$ (cubic) and $Q \rightarrow H_{II}$ transformations. Similar transitions have been observed with N-methyldioleoyl-phosphatidylethanolamine (Siegel & Banschbach, 1990; Siegel, 1986) at 62 °C and 76 ± 4 °C, respectively. A total of 14 CH_2 groups per chain appear to mark a turning point in the transition mechanism. Although the static X-ray pictures in Figure 8 do not show an L_β phase between L_c and L_α, simply because measurements were not performed at intermediate temperatures, synchrotron studies (not shown) reveal the transient appearance of the L_β phase. Actually the transient formation of the L_β phase is also reflected in the strong low-temperature-side asymmetry of the 14-Glc heat capacity curve. For 16-Glc, the stability difference between the L_β and the L_α phase is already so pronounced that a separate peak appears in the heat capacity curve instead of only a low-temperature shoulder. On the other hand, the stability difference between L_α and the H_{II} phase has vanished, as is illustrated by the direct conversion from L_β to H_{II}. Although we did not perform X-ray studies on dispersions of 16-Glc, we have no reason to doubt that 16-Glc exhibits the same thermotropic phase changes as 18-Glc, where they have been identified by small- and wide-angle measurements. With galactolipids the situation is less complex in the first heating, as shown in the top half of Figure 14. Independent of chain length, the transition proceeds from L_c to H_{II}. Thus galactose head groups obviously exert a much stronger influence on the phase behavior. They prevent even lipids with short alkyl chains from populating L_β to L_α phases in the first temperature scan. Time-resolved synchrotron measurements on 14-Gal demonstrated the transient appearance of L_α and L_β on cooling [Quinn, unpublished results cited by Kuttenreich et al. (1988)]. It is therefore tempting to interpret the DSD cooling curve of 14-Gal (Figure 3b) in terms of the phase sequence $H_{II} \rightarrow L_\beta \rightarrow L_c$, where the presumably small volume change associated with the $H_{II} \rightarrow L_\alpha$ transition remained undetected. However, this assignment is at present somewhat speculative and will have to be substantiated by further X-ray studies. The apparent simplicity of the galactolipid transitions is lost after the first heating. The structures assumed on cooling are strongly kinetically determined. As can be seen from the X-ray pattern of 18-Gal, temperature quenching leads to L_β structure while slow cooling

favors formation of the L_c phase. Nevertheless, as can be seen in Figure 14, on the whole the phase behavior of galactolipids as a function of alkyl chain length is less complex than that of the glucolipids.

REFERENCES

Chowdry, B. L., Lipka, G., Dalziel, A. W., & Sturtevant, J. M. (1984) *Biophys. J. 45*, 901–904.

Cuatrecasas, P. (1973) *Biochemistry 12*, 3547–3558.

Curatolo, W. (1987) *Biochim. Biophys. Acta 906*, 137–160.

DeRosa, M., Gambacorta, A., & Gliozzi, A. (1986) *Microbiol. Rev. 50*, 70–80.

Durchschlag, H. (1986) in *Thermodynamic Data for Biochemistry and Biotechnology* (Hinz, H.-J., Ed.) pp 45–128, Springer-Verlag, Berlin.

Epand, R. M., & Epand, R. F. (1980) *Chem. Phys. Lipids 27*, 139–150.

Gounaris, K., Sen, A., Brain, A. P., Quinn, P. J., & Williams, W. P. (1983) *Biochim. Biophys. Acta 728*, 129–139.

Hakamori, S. (1984) *Annu. Rev. Immunol. 2*, 103–126.

Hauser, H., Pascher, I., Pearson, R. H., & Sundell, S. (1981) *Biochim. Biophys. Acta 650*, 21–51.

Haywood, A. M. (1974) *J. Mol. Biol. 83*, 427–436.

Hinz, H.-J., Six, L., Ruess, K.-P., & Lieflander, M. (1985) *Biochemistry 24*, 806–813.

Ishizuka, I., & Yamakava, T. (1985) in *Glycolipids* (Wiegandt, H., Ed.) Elsevier and Academic Press, New York.

Israelachvili, J. N., Mitchell, D. J., & Ninham, B. W. (1976) *J. Chem. Soc., Faraday Trans. 2 72*, 1525–1568.

Israelachvili, J. N., Marcelja, S., & Horn, R. G. (1980) *Q. Rev. Biophys. 13*, 121–200.

Jarrel, C. H., Wand, A. J., Giziewicz, J. B., & Smith, I. C. P. (1987) *Biochim. Biophys. Acta 897*, 69–82.

Koynova, R. D., & Hinz, H.-J. (1990) *Chem. Phys. Lipids 54*, 67–72.

Koynova, R. D., Kuttenreich, H. L., Tenchov, B. G., & Hinz, H.-J. (1988) *Biochemistry 27*, 4612–4619.

Kratky, O., Leopold, M., & Stabinger, H. (1973) *Methods Enzymol. 27*, 98.

Kuttenreich, H., Hinz, H.-J., Inczedy-Marcsek, R., Koynova, R., Tenchov, B., & Laggner, P. (1988) *Chem. Phys. Lipids 47*, 245–260.

Laggner, P., & Stabinger, H. (1976) in *Colloid and Interface Sciences* (Kerner, M., Ed.) Vol. 5, p 91, Academic Press, New York.

Langworthy, T. A., Mayberry, W. R., & Smith, P. F. (1974) *J. Bacteriol. 119*, 106–116.

Langworthy, T. A., Tornabene, T. G., & Holzer, G. (1982) *Zbl. Bakt. Hyg. I. Abt. Orig. C3*, 228–244.

Lis, L. J., Tamura-Lis, W., Lim, T. K., & Quinn, P. J. (1990) *Biochim. Biophys. Acta 1021*, 201–204.

Luzzati, V. (1968) in *Biological Membranes* (Chapman, D., Ed.) pp 71–123, Academic Press, New York.

Maggio, B., Ariga, T., Sturtevant, J. M., & Yu, R. K. (1985) *Biochemistry 24*, 1084–1092.

Mannock, D. A., Brain, A. P., & Williams, W. P. (1985) *Biochim. Biophys. Acta 821*, 153–164.

Mannock, D. A., Lewis, R. N. A. H., Sen, A., & McElhaney, R. N. (1988) *Biochemistry 27*, 6852–6859.

McKeone, B. J., Powell, H. J., & Massey, J. B. (1986) *Biochemistry 25*, 7710–7716.

Nagle, J. F., & Wilkinson, D. A. (1978) *Biophys. J. 23*, 159–175.

Nagle, J. F., & Wiener, M. C. (1988) *Biochim. Biophys. Acta 942*, 1–10.

Pascher, I., & Sundell, S. (1977) *Chem. Phys. Lipids 20*, 175–191.

Privalov, P. L., Plotnikov, V. V., & Filimonov, V. V. (1975) *J. Chem. Thermodyn. 7*, 41–47.

Ruocco, M. J., Siminovitch, D. J., & Griffin, R. G. (1985) *Biochemistry 24*, 2406–2411.

Sastry, P. S. (1974) *Adv. Lipid Res. 12*, 251–310.

Seddon, J. M., Cevc, G., & Marsh, D. (1983) *Biochemistry 22*, 1280–1289.

Sen, A., Williams, W. P., & Quinn, P. J. (1981) *Biochim. Biophys. Acta 663*, 380–389.

Sen, A., Brain, A. P., Quinn, P. J., & Williams, W. P. (1982) *Biochim. Biophys. Acta 686*, 215–224.

Sen, A., Yang, P. W., Mantsch, H. H., & Hui, S. W. (1988) *Chem. Phys. Lipids 47*, 109–116.

Shipley, G. G., Green, J. P., & Nichols, B. W. (1973) *Biochim. Biophys. Acta 311*, 531–544.

Siegel, D. P. (1986) *Chem. Phys. Lipids 42*, 279–301.

Siegel, D. P., & Banschbach, J. L. (1990) *Biochemistry 29*, 5975–5981.

Simmons, K., & van Meer, G. (1988) *Biochemistry 27*, 6197–6202.

Six, L. (1984) Ph.D. Thesis, University of Regensburg.

Six, L., Ruess, K.-P., & Lieflander, M. (1983) *Tetrahedron Lett. 24*, 1229–1232.

Skarjune, R., & Oldfield, E. (1979) *Biochim. Biophys. Acta 556*, 208–218.

Sweeley, C. C., & Siddiqui, B. (1977) in *Glycoconjugates* (Horrewitz, M. J., & Pigman, W., Eds.) Vol. I, pp 459–540, Academic, New York.

Tanford, C. (1972) *J. Phys. Chem. 76*, 3020–3024.

Ward, J. B. (1981) *Microbiol. Rev. 45*, 211–243.

Wiegandt, H. (1985) in *Glycolipids* (Wiegandt, H., Ed.) Elsevier and Academic Press, New York.

Wiener, M. C., Tristram-Nagle, S., Wilkinson, D. A., Campbell, L. E., & Nagle, J. F. (1988) *Biochim. Biophys. Acta 938*, 135–142.

Wieslander, A., Christiannson, A., Rilfors, L., & Lindblom, G. (1980) *Biochemistry 19*, 3650–3655.

Wilkinson, D. A., & Nagle, J. F. (1984) *Biochemistry 23*, 1538–1541.

Womersley, C., Uster, P. S., Rudolph, A. S., & Crowe, J. H. (1986) *Cryobiology 23*, 245–254.